Journal of Cell and Molecular Research (2026) 18 (1), 1-15 DOI: 10.22067/jcmr.2026.92836.1111

Research Article

Bovine Tendon–derived Acellular Matrix Retains Native Extracellular Architecture and Supports Osteogenic and Adipogenic Differentiation of Human Mesenchymal Stem Cells

Mahboubeh Elahifar[1§], Minoo Hosseinimehr[1,2§], Halimeh Hassanzadeh[3], Nasser Mahdavi-Shahri[1], Maryam M. Matin[1,4*]

[1] *Department of Biology, Faculty of Science, Ferdowsi University of Mashhad, Mashhad, Iran*
[2] *Australian Regenerative Medicine Institute, Monash University, Melbourne, Australia*
[3] *Stem Cells and Regenerative Medicine Research Group, Academic Center for Education, Culture and Research (ACECR)-Khorasan Razavi Branch, Mashhad, Iran*
[4] *Institute of Biotechnology, Ferdowsi University of Mashhad, Mashhad, Iran*

Received 30 March 2025 Accepted 13 April 2026

Abstract

Recent advances in stem cell biology and tissue engineering are becoming progressively oriented towards designing natural cellular microenvironments as scaffolds to improve cell growth, differentiation, and functional assembly. Scaffolds are one of the most important components of tissue engineering. Decellularized tissues and organs, either alone or combined with other compositions, have been successfully used as scaffolds in regenerative medicine. The purpose of this study was to fabricate a biological scaffold by decellularizing the bovine tendon as a biomatrix. A biomatrix is a scaffold composed of natural extracellular matrix (ECM) components that are derived from decellularized tissues. The effects of the biomatrix on the growth and differentiation of human adipose-derived mesenchymal stem cells (hAd-MSCs) were then evaluated *in vitro*. The bovine tendon was decellularized by physical, enzymatic, and chemical treatments. Histological staining demonstrated that these treatments successfully removed the cells and cell debris from the tendon, while the conservation of collagen, proteoglycans, glycosaminoglycans, and glycoproteins indicated good preservation of the ECM. Furthermore, cell survival, growth, and differentiation were assessed on the tendon biomatrix. The results indicated that the biomatrix could support the survival and division of hAd-MSCs. Comparison of culture on biomatrix and plastic surfaces indicated significant inductive effects of biomatrix on cell proliferation and on osteogenic and adipogenic differentiation potential. In conclusion, this tendon biomatrix may have useful applications in tissue engineering and regenerative medicine, although further *in vivo* studies are required to prove its efficacy.

***Keywords*:** adipose-derived mesenchymal stem cells, biomatrix, scaffolds, tendon, osteogenic differentiation, adipogenic differentiation

Introduction

Tissue engineering is defined by using three main components: cells, scaffolds, and growth factors for functional tissue/organ formation in therapeutic applications (Atala, 2008; Wang et al., 2021). It requires effective methods to impact various cellular behaviors such as proliferation, migration, and differentiation toward specific phenotypes (Gresham et al., 2021). This technology takes advantage of approaches such as synthetic scaffolds or biomaterial-based techniques (Yang et al., 2025), the use of decellularized natural materials (Shelar et al., 2025), or scaffold-free methodologies; however, the presence of cells is inevitable (Zorlutuna et al., 2013).

Over the past decades, mesenchymal stem cells (MSCs) have raised tremendous expectations as a hopeful cell source for tissue engineering (Ezquer et al., 2017) due to their self-renewal capacity, multilineage differentiation potential, and immunomodulatory properties (Haghighitalab et al., 2021; Kondo et al., 2019). However, directing MSCs toward specific lineages remains a major challenge, particularly in complex tissue environments or under clinical conditions (Jasim et al., 2022).

The extracellular matrix (ECM) is a key regulator of stem cell fate. Acting as a structural scaffold, it contains intrinsic biochemical and

§ Both authors have contributed equally to this work.

* Corresponding author's e-mail address: matin@um.ac.ir

Licensed as Open Access CC-BY

mechanical cues that govern cell survival, growth, and proliferation and can induce changes in cellular morphology, migration, and differentiation. It is also engaged in development, homeostasis, and response to injury. The ECM is composed of structural proteins such as collagen, laminin, and fibronectin, as well as glycoproteins and proteoglycans that form a dynamic 3D microenvironment enabling continuous cell–matrix crosstalk (Nyström & Bruckner-Tuderman, 2019; Sarangthem et al., 2022; Wen et al., 2020). Recent studies demonstrate that physical forces like ECM stiffness can also modulate cellular metabolism and mechanotransduction cascades, thereby influencing lineage specification and matrix remodeling, features that can be precisely tuned for regenerative medicine applications (Kersey et al., 2024; Na et al., 2024). Thus, reproducing the biochemical composition and mechanical properties of native ECM is crucial for scaffold design in functional tissue regeneration (Guo et al., 2021).

Biomatrix is composed of natural ECM components derived from decellularized tissues and provides a suitable microenvironment for stem cells. In different studies, a wide range of tissues have been used to prepare decellularized ECM (dECM), such as heart valves (Bai et al., 2022; Lichtenberg et al., 2006), skin (Kamalvand et al., 2021; Pesaraklou et al., 2019), aorta (Giovanniello et al., 2023; Kazemi et al., 2021), amniotic membrane (Iranpour et al., 2018), skeletal muscle (Porzionato et al., 2015), bone (Shahabipour et al., 2013), and articular cartilage (Ghassemi et al., 2017; Luo et al., 2015). The physical, biological, and chemical characteristics of dECM influence its properties, which can vary with the tissue source and decellularization method used (Milan et al., 2020). Native ECM possesses intrinsic signals that can facilitate cell attachment, proliferation, and differentiation, thereby promoting tissue regeneration (Hsieh et al., 2021; Song & Ott, 2011). Given the scarcity of human tissues, xenogeneic sources, such as bovine tissues, offer an accessible and reliable alternative for scaffold fabrication (Casarin et al., 2022; Tavassoli et al., 2015).

In this study, we fabricated a bovine tendon-derived acellular matrix with well-preserved extracellular components and evaluated its effects on the proliferation and osteogenic and adipogenic differentiation of human adipose-derived MSCs (Ad-MSCs). This work aims to introduce a natural, xenogeneic scaffold with favorable properties for stem cell–based regenerative applications.

Materials and Methods

Biomatrix fabrication and histological assessment of decellularization

To prepare a biomatrix from the ECM, bovine-derived tendons were washed with phosphate-buffered saline (PBS) and then sliced into 2×2 mm pieces. The pieces of tendon were then decellularized using physical, enzymatic, and chemical treatments. Physical decellularization was performed with snap freeze-thaw repeated 5 times (Jackson et al., 1988; Roth et al., 2018). For enzymatic treatment, tendons were placed in a 0.5% trypsin/PBS solution (prepared by dissolving 0.5 g trypsin in 100 ml PBS; Gibco) and incubated at 37ºC for 24 h, with the trypsin solution replaced every 4 h. This step was followed by three PBS washes, each for 30 min (Yang et al., 2010). Chemical treatment was performed using a 1% Triton X-100 (Cinnagen) solution, prepared by adding 1 ml of Triton X-100 to 100 ml of PBS, and the samples were incubated for 24 h to complete the decellularization process (Shahraki et al., 2022; Zhang et al., 2011). One gram of tendon matrix was dissolved in 3 ml 0.3% acetic acid (Merck) and spread on the surfaces of 6-well plates in sterile condition followed by 12 h exposure to ultraviolet (UV) light (Figure 1). The prepared biomatrix, attached to 6-well plates, was washed three times with PBS, five times with 70% ethanol, and three times with PBS to make it ready for cell culture. Commonly accepted metrics for assessing decellularization include Hematoxylin and Eosin (H&E) (Merck) and 4′, 6-diamidino-2-phenylindole (DAPI) (Merck) staining to verify the absence of cells and cell nuclei and to assess the reduction in the amount and length of double-stranded genomic DNA (Crapo et al., 2011; Jambar Nooshin et al., 2023).

The efficiency of cell removal and collagen conservation was assessed in decellularized tendons using histological staining (Kiernan, 2008). For this purpose, before the addition of acetic acid, samples were fixed in 3.7% formalin (Asia Pajuhesh) for 3 days, followed by dehydration through a series of graded ethanol (50%, 12 h) (70%, 12 h) (90%, 8 h) and butanol (Merck) for 12 h. Sections were prepared from paraffin-embedded samples (Merck), dewaxed, and stained accordingly. Cell removal was studied with H&E (Lillie et al., 1976) and also DAPI staining (Kapuscinski, 1995). Collagen conservation analysis was performed with Picrosirius Red (PSR) (Merck), Van Gieson (Merck), and Carmine-picroindigocarmine (Merck), accompanied by Weigert Hematoxylin staining (Junqueira et al., 1982).

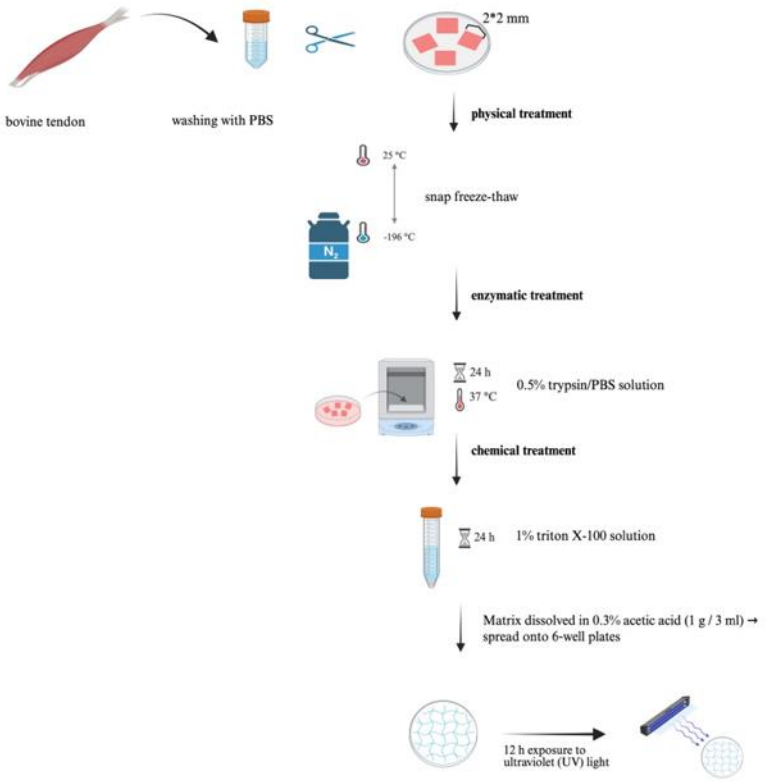


Figure 1. Schematic illustration of bovine tendon decellularization and biomatrix preparation. The figure illustrates the stepwise procedure for preparing the extracellular matrix-derived biomatrix from bovine tendons. Bovine tendons were first washed with phosphate-buffered saline (PBS) and cut into 2×2 mm pieces. Physical decellularization was performed by snap freeze-thaw cycles repeated five times. Enzymatic treatment involved incubation in 0.5% trypsin in PBS at 37°C for 24 h. Chemical decellularization was performed with a 1% Triton X-100 solution for 24 h. Finally, 1 g of decellularized tendon matrix was dissolved in 3 ml of 0.3% acetic acid, spread onto 6-well plates under sterile conditions, and exposed to 12 h of ultraviolet (UV) light to prepare the biomatrix for subsequent cell culture experiments.

Finally, to assess the maintenance of carbohydrate-rich ECM components, including proteoglycans, glycosaminoglycans, and glycoproteins, Periodic acid–Schiff (PAS)–Hematoxylin–Picroindigocarmine staining (all from Merck) was performed. In this procedure, periodic acid oxidizes carbohydrate vicinal diols to aldehyde groups, which then react with Schiff's reagent to produce a purple color, enabling visualization of sugar-containing structures and confirming preservation of these components in the decellularized tendon tissue (Junqueira et al., 1998).

Mesenchymal stem cell isolation and characterization

In order to derive mesenchymal stem cells, adipose tissue was obtained from healthy women undergoing elective liposuction. MSCs employed in this study were previously isolated under an ethics approval obtained for another research project (IR.ACECR.JDM.REC.1397.008). Written informed consent was obtained from all donors, allowing the use of their biological samples for research purposes. The lipoaspirates were minced and washed three times with PBS containing penicillin–streptomycin (Biowest). Then, samples were digested with 0.1% collagenase type I (Gibco) at 37ºC for 1 h. They were gently agitated manually every 5-10 min to enhance digestion efficiency. The enzyme was then inactivated by the addition of 10% fetal bovine serum (FBS, Biowest), followed by centrifugation (Orto Alresa Digicen, Spain) at 800 *g* for 10 min. The pellet containing MSCs was resuspended in Dulbecco's modified Eagle's medium (DMEM, Gibco) supplemented with 10% FBS, 100 U/ml penicillin, and 100 µg/ml streptomycin and cultured in T25 culture flasks (Naderi-Meshkin et al., 2016). The medium was

replaced after 48 h to remove non-adherent hematopoietic cells and debris, and upon reaching 90% confluency, cells were passaged using 0.25% trypsin/1 mM ethylenediaminetetraacetic acid (EDTA) (Gibco). Cells at passages 3-4 were used for further experiments. MSCs were characterized according to the minimal criteria proposed by the International Society for Cellular Therapy (ISCT) in 2006, including plastic adherence under standard culture conditions, expression of specific surface markers such as CD90, lack of hematopoietic markers, including CD34 and CD11b, as well as their differentiation potential. Although CD44 is not included in the ISCT minimal criteria, it is recognized as a classical and consistently expressed MSC marker (Dominici et al., 2006; Santoro et al., 2025). In the present study, the obtained cells were characterized by verifying their morphology, marker expression, and multipotent differentiation potential. The expression of the following cell surface markers was analyzed by flow cytometry: CD90 and CD44 as positive and CD34 and CD11b as negative markers. The antibodies used included a mouse anti-CD90 monoclonal antibody, mouse anti-CD44 polyclonal antibody, rabbit anti-CD34 polyclonal antibody, and rabbit anti-CD11b polyclonal antibody (all from Cytognos, Spain). To do so, trypsinized cells were washed twice with PBS and resuspended in PBS containing 0.5% FBS. 100 µl of cell suspension was then incubated with different antibodies for 45 min at room temperature in the dark. An isotype control for each antibody was also applied to the cells to help the gating process. Data were acquired using a flow cytometer (BD Accuri C6, USA) and analyzed with FlowJo software (version 7.6.1). The differentiation potential of the cells towards osteoblasts and adipocytes was investigated through incubation in specific induction media for 21 and 17 days, respectively. The osteogenic medium was composed of DMEM supplemented with 10% FBS, 1 µM dexamethasone, 10 mM β-glycerol phosphate, and 20 µM ascorbic acid; and the adipogenic medium included DMEM supplemented with 10% FBS, 1 µM dexamethasone, 10 mM β-glycerol phosphate and 100 µM indomethacin (all reagents were from Sigma). Osteogenesis and adipogenesis were assessed using Alizarin Red S (ARS, Sigma) and Oil Red O (ORO, Sigma) staining, respectively (da Silva Meirelles et al., 2008; Naderi-Meshkin et al., 2016).

Investigating the effects of biomatrix on MSC growth and differentiation

Population doubling time (PDT)

Ad-MSCs at passage 4 were seeded in 6-well plates at a density of 0.1×10^5 cells/cm^2 either with or without biomatrix. After 48 h, cells were harvested by trypsin-EDTA and counted. Population doubling time (PDT) was calculated using the following formula (Piera-Velazquez et al., 2002):

$$PDT=CT/\log N/N0\times 3.31$$

(CT: culture time; N0: number of seeded cells; N: number of counted cells)

Osteogenic and adipogenic differentiation

In order to check the effects of biomatrix on the differentiation of Ad-MSCs, cells were cultured in 6-well plates with or without biomatrix. Differentiation induction was performed using osteogenic and adipogenic media, as previously described (da Silva Meirelles et al., 2008; Naderi-Meshkin et al., 2016) for 7, 14, and 21 days. Ad-MSCs cultured on biomatrix without induction media were also used as controls.

Qualitative evaluation of osteogenesis (mineralization assay)

Mineralization, or the formation of calcium deposits, represents the final step of osteogenesis. *In vitro* mineralization was verified by Alizarin Red S staining. To perform this procedure, osteogenic medium was removed, and cells were washed twice with PBS and fixed by covering with 10% (v/v) formaldehyde at room temperature. After 15 min of fixation, cells were rinsed twice with distilled water and stained with 1 ml/well of 40 mM ARS (pH 4.1) for 20 min with gentle shaking, followed by washing with distilled water (Gregory et al., 2004). Ad-MSCs cultured on biomatrix without induction medium were also used as a control.

Quantitative evaluation of osteogenesis

Matrix mineralization on the biomatrix and plastic surfaces of 6-well plates was quantified by extracting ARS after 7, 14, and 21 days. To do so, acetic acid (800 µl, 10% v/v) was added to the stained samples and incubated with shaking (Sci Finetech, Korea) at room temperature for 30 min, followed by scraping the cells and transferring them to 1.5 ml microtubes. Then, it was vortexed (Stuart, UK) for 30 s, overlaid with 500 µl mineral oil to prevent evaporation, and heated at 85ºC for 10 min, and then transferred on ice for 5 min. After that, samples were centrifuged at 20000 *g* for 15 min. The pH of the supernatant was adjusted to 4.1-4.5 with ammonium hydroxide (10% v/v) followed by the colorimetric detection at 405 nm (ELISA reader, StatFax, Germany) (Gregory et al., 2004). At least three independent experiments were performed, each one in triplicate.

Qualitative evaluation of adipogenesis

Intracellular lipids as a marker for adipogenesis were visualized by Oil Red O staining (Kuhbier et al., 2010). To do so, the adipogenic medium was removed, and cells were washed twice with PBS and fixed in 10% formalin for 5 min. After that, cells were incubated with 60% isopropanol (Merck) for 5 min, followed by ORO staining for 10 min and washing with distilled water (dH_2O) (Ramírez-Zacarías et al., 1992). Ad-MSCs cultured on biomatrix without induction medium were also used as a control.

Quantitative evaluation of adipogenesis

Intracellular lipid production in cells cultured on biomatrix and plastic surfaces of 6-well plates was quantified by extracting ORO after 7, 14, and 21 days. Extracted ORO was eluted by adding 100% isopropanol and incubating for 10 min. After that, extracted stains were transferred to 1.5 ml microtubes and their optical density (OD) was measured at 510 nm. For this purpose, at least three independent experiments were performed, each one in triplicate.

Statistical analyses

Data normality was assessed prior to statistical analysis. Comparisons among multiple groups were performed using one-way analysis of variance (ANOVA), followed by Tukey's post hoc test for multiple comparisons. For proliferation analysis, to examine the capacity of the biomatrix to support cell attachment and maintenance *in vitro*, comparisons between two groups were performed using a two-tailed Student's *t*-test. Experiments were repeated at least three times. Statistical analyses were conducted using GraphPad InStat version 10.2.0 (GraphPad Software, San Diego, CA, USA). Data are presented as mean ± standard deviation (SD), and differences were considered statistically significant at $p < 0.05$.

Results

Fabrication and histological evaluation of the tendon-derived biomatrix

The biomatrix was fabricated efficiently from the ECM of bovine tendon (Figure 1). Histological studies demonstrated that physical, enzymatic, and chemical treatments have removed the cells from bovine tendon, and conservation of collagens, proteoglycans, glycosaminoglycans, and glycoproteins indicated good preservation of the ECM, as shown in Figure 2. Cell removal was confirmed by H&E staining (Figure 2, a and b), and DAPI staining was also performed to confirm removing the nuclei and chromatin components from decellularized tendon. In this staining, nuclei and DNA can be observed under fluorescence microscopy, as shown in Figure 2c and d. In order to check the integrity of the ECM after the decellularization process, different staining protocols were performed, including Picrosirius Red, which is one of the best histochemical methods for analyzing collagen content, and stains thick collagen bundles red and thin collagen fibrils in yellow or green (Figure 2, e and f). Collagen was stained greenish blue by Picroindigocarmine (Figure 2, g and h). Van Gieson or Picrofuchsin is a highly acidic color, which stains connective tissue containing collagens as pink, while cytoplasm, muscles, fibrin, and erythrocytes appear yellow (Figure 2, i and j). Hematoxylin Weigert stains cell nuclei dark violet and chromatin black or blue (Junqueira et al., 1982). All these different staining methods showed that collagen was conserved after the decellularization process. PAS especially stains proteoglycans, glycosaminoglycans, and glycoproteins purple (Figure 2, k and l). Our results confirmed the maintenance of these components in the epitenon and endotenon of the tendon after the decellularization procedure.

Isolation and characterization of adipose-derived mesenchymal stem cells

Flow cytometry analysis indicated that isolated cells were mostly positive for CD90 and CD44, while they did not express CD34 and CD11b cell surface markers (Figure 3A).

Differentiation potential towards osteogenic and adipogenic lineages was shown through Alizarin Red S and Oil Red O staining, respectively (Figure 3B), and both assays confirmed the identity of isolated cells as MSCs. After confirming the identity of Ad-MSCs, they were cultured on the fabricated tendon biomatrix to evaluate how this native scaffold influences their biological behavior, including cell proliferation and differentiation potential.

Effects of tendon biomatrix on Ad-MSC behavior

***Proliferation analysis*:** To examine the capacity of the biomatrix to support cell attachment and maintenance *in vitro*, Ad-MSCs were seeded at a density of 10^4 cells/cm^2 either on the biomatrix or on a plastic surface. Cells could normally adhere to the biomatrix, indicating the capacity of the bovine tendon biomatrix for culturing mesenchymal stem cells. PDT analysis showed that cells cultured on biomatrix had a PDT of 30 h, compared to 48 h on plastic surface (Table S1), indicating that the biomatrix provided a more supportive microenvironment for MSC proliferation.

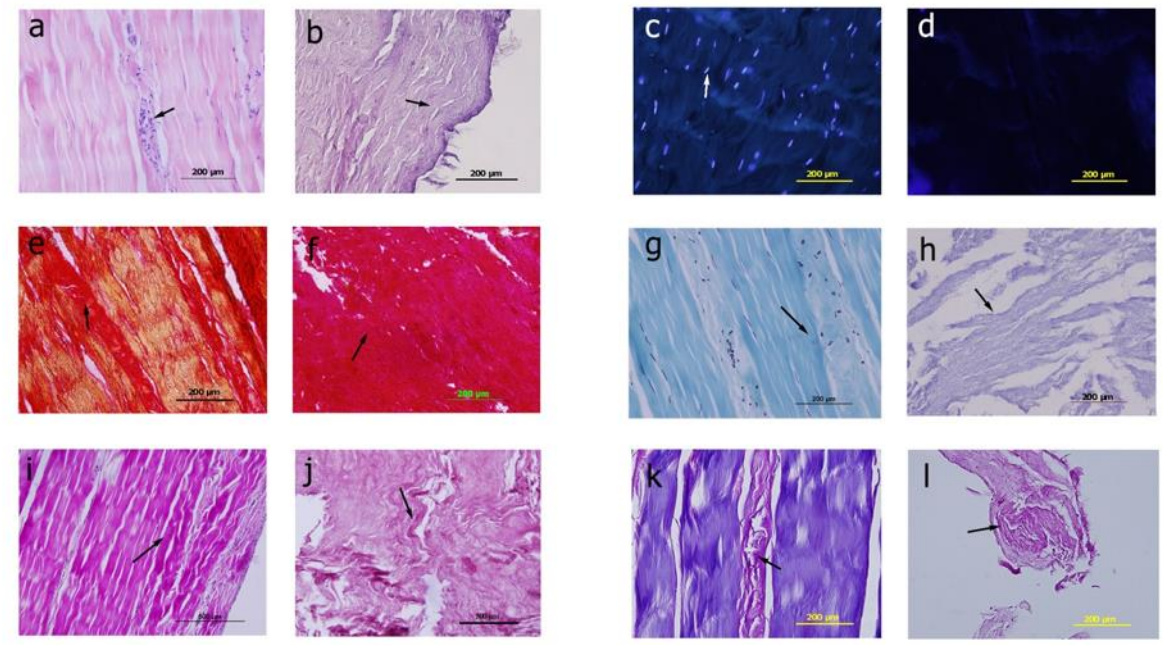


Figure 2. Evaluation of cell removal and preservation of collagen and natural sugar components in decellularized tendon by histological staining. a, c, e, g, i and k: Normal tendon; b, d, f, h, j and l: Decellularized tendon. a and b are stained with H & E, in which nuclei and other basophilic structures are purple (arrow in a), and cytoplasm and acidophilic structures are stained light to dark pink (arrow in b); c and d: DAPI staining shows cell nuclei as bright blue (arrow in c). After decellularization (d), the absence of nuclear staining confirms the effective removal of cells. To analyze the integrity of the ECM in normal and decellularized tendon, additional methods were also employed. e and f: Picrosirius Red stains thick collagen bundles red (arrow) and thin collagen fibrils in yellow or green. g and h: After Picroindigocarmine staining, collagen appears as greenish blue (arrow); i and j: collagen after Van Gieson staining is pink (arrow). These pictures indicate that collagen was preserved after the decellularization procedure. k and l: Investigating the maintenance of natural sugar components in decellularized tendon using PAS staining. Purple color represents the existence of natural sugar components (arrow); Scale bars: 200 µm (a–h, k–l); 500 µm (i–j).

PDT=CT/log N/N0×3.31

CT: culture time; N: number of counted cells; N0: number of seeded cells

Without biomatrix: PDT=48/log (200000/100000) ×3.31=48.192

Using biomatrix: PDT=48/log (300000/100000) ×3.31=30.37

These findings indicate that the tendon biomatrix significantly enhanced MSC proliferation compared with the standard plastic surface.

***Osteogenic differentiation of Ad-MSCs on the biomatrix*:** Osteogenic differentiation potential of Ad-MSCs was examined by culturing the cells in osteogenic induction medium. It was hypothesized that, due to the presence of proteoglycans, glycosaminoglycans, and collagen in the biomatrix and their effects in accelerating osteogenesis, growth on the biomatrix would increase their differentiation potential. Qualitative and quantitative assessments of osteogenesis were conducted simultaneously. Calcium secretion and deposition in the ECM represent osteoblast differentiation *in vitro*, which can be identified specifically by ARS that stains calcium red or light orange. Qualitative investigation displayed no Ad-MSC differentiation into osteoblasts after 7 days in samples cultured in untreated 6-well plates, whereas Ad-MSCs on biomatrix showed osteoblast differentiation within the same time interval. Therefore, biomatrix accelerated osteogenesis in comparison with the plastic surface of 6-well plates (Figure 4A). The deposit of extracellular calcium and the number of differentiated osteoblasts increased over time in both groups; however, at all-time points, differentiated Ad-MSCs and extracellular calcium on the biomatrix were greater than in untreated 6-well plates (Figure 4A). Quantitative analysis of ARS extraction and absorbance at 405 nm confirmed that the biomatrix accelerated osteogenic differentiation compared with the control (Figure 4B) (Table S2).

***Adipogenic differentiation of Ad-MSCs on the biomatrix*:** To determine the effects of tendon biomatrix on adipogenesis, production of

intracytoplasmic triglycerides was evaluated in cells cultured on biomatrix and plastic surfaces in the presence of adipogenic induction medium. Synthesis and storage of triglycerides in adipocytes can be specifically identified by ORO, which stains the triglycerides in red, and its OD is used for quantitative determination of adipogenesis (Table S3). After 7 days, observation of red lipid droplets in cells grown on biomatrix and the lack of lipid droplets in control cells grown on a plastic surface indicated that adipogenic differentiation of Ad-MSCs was accelerated on biomatrix (Figure 5A). Evaluations on days 7, 14, and 21 after induction of adipogenesis in the presence and absence of biomatrix showed that cytoplasmic triglycerides and the number of cells differentiated into adipocytes increased over time in both groups, while culture on biomatrix significantly enhanced differentiation at each time point. Quantitative measurement of extracted ORO showed that triglyceride accumulation increased over time in both groups but significantly more in cells cultured on the biomatrix (Figure 5B). The results demonstrated that tendon biomatrix enhanced Ad-MSC differentiation to adipocytes.

Discussion

In this study, a thin layer of decellularized tendon matrix, or tendon biomatrix, was fabricated by snap freeze-thaw, followed by treatments with trypsin, Triton X-100, and acetic acid as physical, enzymatic, and chemical decellularization methods, respectively (Figure 1). We attempted to choose methods that have the least detrimental effects on ECM components and could effectively remove cells and cell debris.

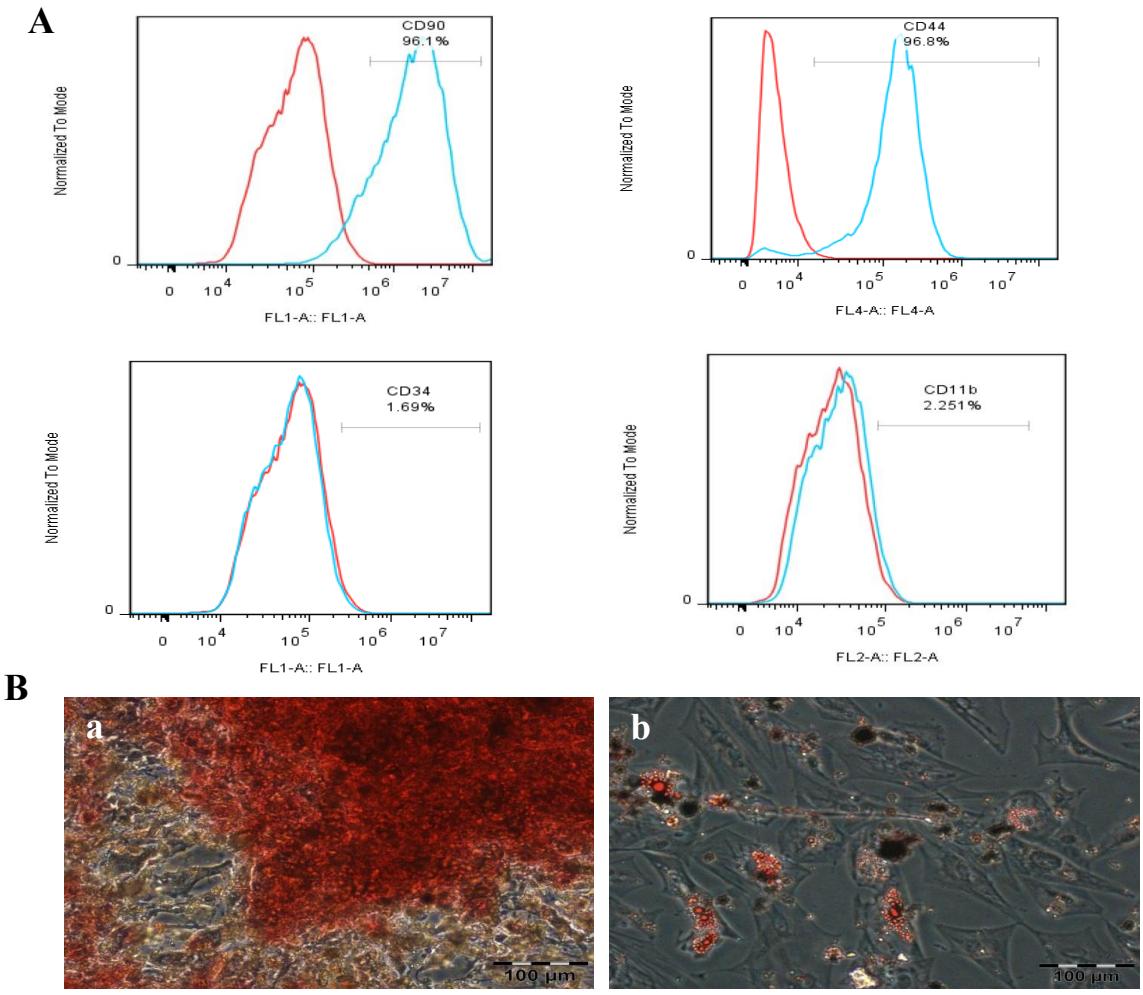


Figure 3. Characterization of human Ad-MSCs. (A) Flow cytometric analysis confirmed expression of MSC surface markers: CD90 (96.1%) and CD44 (96.8%) were positive, whereas hematopoietic markers CD34 (1.6%) and CD11b (2.2%) were negative. (B) Multipotent differentiation of Ad-MSCs was demonstrated by a) Osteogenic differentiation (Alizarin Red S staining of calcium deposits) and b) Adipogenic differentiation (Oil Red O staining of lipid droplets) (scale bars: 100 µm).

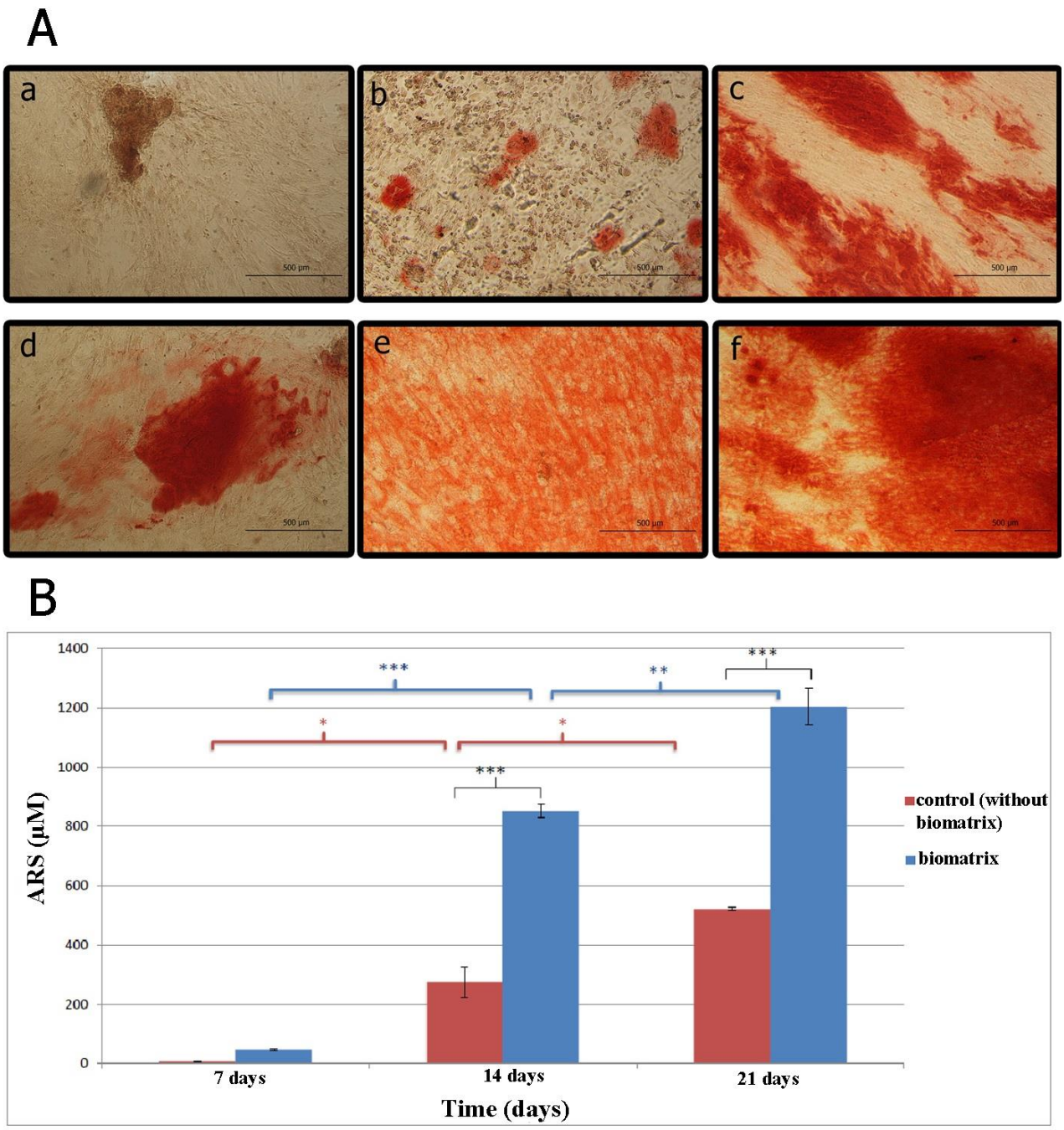


Figure 4. Biomatrix supported osteogenic differentiation of Ad-MSCs during 21 days of culture. A) Cells cultured on biomatrix showed enhanced differentiation into osteoblasts, as indicated by increased calcium deposition stained red with Alizarin Red S. Ad-MSCs were cultured on 6-well plates without biomatrix (a, b, c) or with biomatrix (d, e, f). Pictures were taken at three time points: after 7 days (a and d), 14 days (b and e), and 21 days (c and f); scale bars: 500 µm. B) Quantitative evaluation of osteogenesis. As shown, biomatrix increased the osteogenesis potential of Ad-MSCs. Data are presented as mean ± SD of at least three independent experiments (*$p < 0.05$, **$p < 0.01$ and ***$p < 0.001$).

Unlike other methods in which extracting collagen from the tendon or other tissues is performed by grinding the tissues into powder (Chen et al., 2023), here sliced tendon tissues were used in order to preserve their natural microstructure. The tendon consists of hierarchical layers, including the epitenon, a connective tissue sheath surrounding the tendon, and the endotenon, which separates collagen bundles (Bordoni et al., 2025); preservation of these structures likely contributes to the biomatrix mechanical and biological functionality.

Trypsin was used for enzymatic decellularization because it cleaves the peptide bond on the carboxyl side of arginine and lysine in the absence of proline. For structural reasons, collagen fibers might have relative resistance to trypsin (Waldrop et al., 1980). Triton X-100 is a nonionic detergent that does not affect conserved protein–protein interactions and their structural features (Seddon et al., 2004).

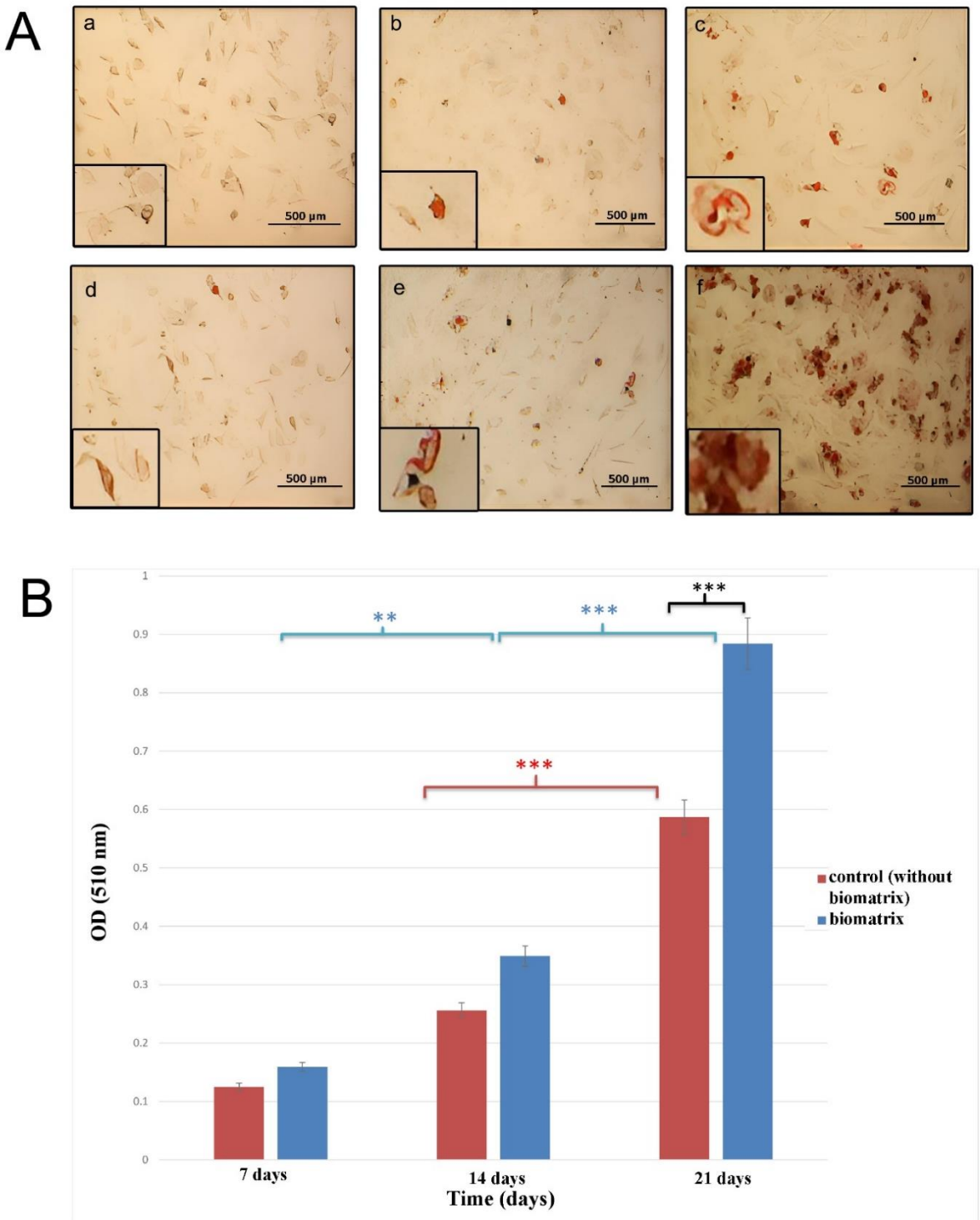


Figure 5. Biomatrix-supported adipogenic differentiation of Ad-MSCs during 21 days of culture. A) Cells on biomatrix showed stronger adipogenic differentiation with greater accumulation of cytoplasmic triglycerides stained red with Oil Red O. Ad-MSCs cultured on 6-well plates without biomatrix (a, b, c) or with biomatrix (d, e, f). Pictures were taken at three time points: after 7 days (a and d), 14 days (b and e), and 21 days (c and f); scale bars: 500 µm. B) Quantitative evaluation of adipogenesis. As shown, biomatrix increased the adipogenesis potential of Ad-MSCs. Data are presented as mean ± SD of at least three independent experiments (**$p < 0.01$ and ***$p < 0.001$).

Eventually, treatment with acetic acid results in rearrangement of intermolecular bonds in collagens (Lian et al., 1973). Preparing a biomatrix, rather than using only a decellularized tendon specimen as a scaffold (Khakpour et al., 2023), was promising for maintaining the matrix and improving its functionality.

H&E and DAPI staining methods confirmed the removal of cells and cell debris from the tendon tissue (Figure 2). Specific staining techniques, including Picrosirius Red, Van Gieson's Picrofuchsin, and Indigocarmine, confirmed that collagens were preserved after decellularization process. Furthermore, utilization of Weigert's Hematoxylin also disclosed that tendon matrix decellularization was perfectly applied (Figure 2). Similarly, PAS staining demonstrated that during decellularization of tendon tissue, natural sugar compounds such as proteoglycans, glycosaminoglycans, and glycoproteins remained mainly intact (Figure 2). These results demonstrate that our multi-step protocol effectively removed cellular debris without compromising ECM components critical for various cellular responses.

Ad-MSCs are highly suitable for studies involving decellularized biomatrices due to their intrinsic capacity for proliferation, multilineage differentiation, and immunomodulatory properties, which are advantageous for tissue regeneration (Gou et al., 2024). They proliferate rapidly *in vitro*, making them ideal for testing the biological functionality of a new biomatrix (Zhang et al., 2015). When cultured on decellularized ECM, Ad-MSCs more effectively mimic the native tissue microenvironment, thereby promoting cellular attachment, proliferation, and differentiation into desired cell types (Stukel Shah et al., 2022). Moreover, these cells express integrins and adhesion molecules that interact with ECM components such as collagen I, fibronectin, and laminin, which are abundant in the bovine tendon–derived matrix (Wang et al., 2020). These properties make them a good biological model for assessing biocompatibility and bioactivity of ECM scaffolds. Furthermore, adipose tissue is readily available and can be harvested with minimal invasiveness, rendering Ad-MSCs more clinically accessible than other cells (Kostecka et al., 2024).

Accurate identification of MSCs is essential for ensuring reproducibility, and recent advances in surface marker profiling and characterization technologies have improved the standardization and accuracy of MSC identification (Santoro et al., 2025). Flow cytometry analysis confirmed the mesenchymal identity of the isolated cells. Ad-MSCs showed strong expression of CD90 and CD44, two characteristic MSC markers (Camilleri et al., 2016), and were negative for the hematopoietic markers CD34 and CD11b (Figure 3A). This expression pattern, together with their fibroblast-like morphology, validated the mesenchymal nature of the isolated cells. Regulating stem cell proliferation is an essential feature of the niche (Fuchs et al., 2004). In this study, the tendon-derived biomatrix provided a more physiologically relevant microenvironment for Ad-MSCs compared with standard tissue-culture plastic surfaces. Cells cultured on the biomatrix exhibited a shorter PDT, indicating that the matrix better supported their proliferation. This enhancement likely arises from cell–matrix interactions that replicate native extracellular signals, facilitating adhesion, survival, and balanced proliferation. Moreover, when Ad-MSCs were cultured on the biomatrix in the absence of induction media, they maintained their stem cell characteristics, confirming that the scaffold sustained their normal self-renewal potential without promoting spontaneous differentiation.

Differentiation potential towards osteoblasts is a fundamental property of Ad-MSCs (Mo et al., 2016). Osteoblasts are specialized cells that are able to secrete a mineral matrix that consists of type I collagen, Osteocalcin (OC), Osteopontin (OPN), bone sialoprotein (BSP), and minerals (Carvalho et al., 2021; Fantner et al., 2007; Ritter et al., 1992). It has also been shown that Runt-related transcription factor 2 (RUNX2) is a pivotal transcription factor during bone formation, influencing osteoblast differentiation and mineralization. In other words, it affects downstream genes essential to osteoblast phenotype and function (Komori, 2025). Various studies have reported that increasing the expression of these factors promotes osteogenesis and bone healing (Kim et al., 2023). Common methods for assessing osteogenesis and *in vitro* bone formation include analysis of specialized bone tissue markers, such as OC, type I collagen, and mineralization. Mineralization can be evaluated using calcein fluorescence, von Kossa staining, and ARS staining. Von Kossa and ARS staining facilitate the evaluation of mineral dispersion by light microscopy.

Here, Ad-MSCs were cultured in the presence and absence of tendon biomatrix. Cells were treated with osteogenic differentiation medium when they reached 70-80% confluency. After 7, 14, and 21 days, ARS staining, which correlates with mineralization, was performed and quantified as described by Gregory and colleagues (Gregory et al., 2004). Interestingly, both qualitative and

quantitative methods, evaluating osteoblast differentiation, revealed that cells cultured on tendon biomatrix were stained by ARS after 7 days, indicating that the cells had progressed to the matrix mineralization stage of osteogenesis. However, no matrix mineralization was observed in cells cultured on a plastic surface (Figure 4). Qualitative and quantitative methods measuring osteoblast differentiation at days 7, 14, and 21 demonstrated that more osteogenesis occurred in cells grown on the tendon biomatrix than in the control groups. These results indicate that the tendon biomatrix accelerates Ad-MSC osteogenesis compared with a plastic surface. Considering that collagen is expressed from the beginning of osteogenesis as well as initiating matrix mineralization with the deposition of calcium on collagen filaments, tendon biomatrix increases the potential of osteogenesis and accelerates the bone formation process due to its large amount of collagen (Figure 4). Osteogenesis is also augmented as the proteoglycans and glycoproteins that have high affinity for calcium are maintained in the tendon biomatrix (Figure 2). Moreover, external environmental factors for cell-cell and cell-matrix signals that play a dramatic role in condensation of mesenchymal cells and regulate expression of SOX9 and RUNX2 might have accelerated osteogenesis (Ono et al., 2021). Thus, cell-cell and cell-matrix interactions could have a moderate impact on the increased osteogenesis in a biomatrix.

To assess the effects of the tendon biomatrix on the differentiation potential of Ad-MSCs, adipogenesis was evaluated by assessing intracytoplasmic triglycerides. Ad-MSCs were cultured either on a biomatrix or on a plastic surface, and when they reached 70-80% confluency, cells were treated with adipogenic differentiation medium. Adipogenesis was verified after 7, 14, and 21 days by Oil Red O staining followed by light microscopy. Moreover, ORO was extracted with isopropanol, and its absorbance was measured at 510 nm (Ramírez-Zacarías et al., 1992). Qualitative and quantitative results showed that in both groups, the number of differentiated cells with intracytoplasmic triglycerides increased over time, whereas at each time point, more adipogenic differentiation was observed on the biomatrix (Figure 5). Similar to osteogenic differentiation, 7 days after treatment, adipocytes could be detected only in induced cells cultured on biomatrix. Hence, biomatrix enhanced both osteogenic and adipogenic differentiation potentials of human Ad-MSCs. Furthermore, alterations in lipid synthesis led to changes in the ECM during adipocyte differentiation. A previous study showed that the levels of eight ECM proteins increased 3-6-fold under adipogenic conditions (Nakajima et al., 2002). The synthesis and secretion of ECM components are increased during adipocyte differentiation (Soták et al., 2022). Similarly, immunocytochemical staining revealed the organization of fibrous networks composed of type I, III, V, and VI collagens in primary cultures during adipocyte differentiation (Kubo et al., 2000).

In this study, we developed a new decellularization protocol that integrates physical, enzymatic, and chemical treatments to fabricate a bovine-derived tendon scaffold while minimizing disruption of the native ECM architecture and composition. Each of these methods has distinct advantages; by combining them, we aimed to capitalize on their complementary effects to achieve efficient cell removal while preserving the biochemical integrity and mechanical properties of the tendon. This optimized protocol provides a reproducible and effective approach for generating tendon-derived biomatrices suitable for cell-based tissue engineering applications. Compared with previous reports that used ground tendon scaffolds or chemically extracted collagen, our approach uniquely preserved the aligned fibrillar structure of the native tendon ECM. This preservation may explain the superior support for cell proliferation and differentiation observed in our system. Furthermore, the use of a xenogeneic bovine tendon source, combined with human Ad-MSCs, provides an informative and translationally relevant model for future tissue-engineering applications.

Acknowledgments

This work was supported by Ferdowsi University of Mashhad under Grant No. 22848.

We would like to thank Dr. Hojjat Naderi-Meshkin and Mr. Mohammad Nakhaei for their expert technical assistance in this study.

Conflict of Interests

The authors declare that they have no conflicts of interest.

References

Atala, A. (2008). Advances in tissue and organ replacement. Current Stem Cell Research & Therapy, 3(1), 21-31.

Bai, P., Kong, G., Qiao, W., Song, Y., Wang, Y., Shi, J., et al. (2022). A novel method to improve the physical property and biocompatibility of decellularized heart valve scaffold with sericin and

polydopamine. Journal of Bionic Engineering, 19(4), 1109-1123.

Bordoni, B., Black, A. C., & Varacallo, M. A. (2025). Anatomy, Tendons. In StatPearls. StatPearls Publishing Copyright © 2025, StatPearls Publishing LLC.

Camilleri, E. T., Gustafson, M. P., Dudakovic, A., Riester, S. M., Garces, C. G., Paradise, et al. (2016). Identification and validation of multiple cell surface markers of clinical-grade adipose-derived mesenchymal stromal cells as novel release criteria for good manufacturing practice-compliant production. Stem Cell Research & Therapy, 7(1), 107.

Carvalho, M. S., Cabral, J. M. S., da Silva, C. L., & Vashishth, D. (2021). Bone matrix non-collagenous proteins in tissue engineering: creating new bone by mimicking the extracellular matrix. Polymers, 13(7), 1095.

Casarin, M., Fortunato, T. M., Imran, S., Todesco, M., Sandrin, D., Borile, G., et al (2022). Porcine small intestinal submucosa (SIS) as a suitable scaffold for the creation of a tissue-engineered urinary conduit: decellularization, biomechanical and biocompatibility characterization using new approaches. International Journal of Molecular Sciences, 23(5), 2826.

Chen, Y., Chen, L. F., Wang, Y., Duan, Y. Y., Luo, S. C., Zhang, J. T., et al. (2023). Modeling dECM-based inflammatory cartilage microtissues in vitro for drug screening. Composites Part B: Engineering, 250, 110437.

Crapo, P. M., Gilbert, T. W., & Badylak, S. F. (2011). An overview of tissue and whole organ decellularization processes. Biomaterials, 32(12), 3233-3243.

da Silva Meirelles, L., Caplan, A. I., & Nardi, N. B. (2008). In search of the in vivo identity of mesenchymal stem cells. Stem Cells, 26(9), 2287-2299.

Dominici, M., Le Blanc, K., Mueller, I., Slaper-Cortenbach, I., Marini, F., Krause, D., et al. (2006). Minimal criteria for defining multipotent mesenchymal stromal cells. The International Society for Cellular Therapy position statement. Cytotherapy, 8(4), 315-317.

Ezquer, F., Bahamonde, J., Huang, Y. L., & Ezquer, M. (2017). Administration of multipotent mesenchymal stromal cells restores liver regeneration and improves liver function in obese mice with hepatic steatosis after partial hepatectomy. Stem Cell Research & Therapy, 8(1), 20.

Fantner, G. E., Adams, J., Turner, P., Thurner, P. J., Fisher, L. W., & Hansma, P. K. (2007). Nanoscale ion mediated networks in bone: osteopontin can repeatedly dissipate large amounts of energy. Nano Letters, 7(8), 2491-2498.

Fuchs, E., Tumbar, T., & Guasch, G. (2004). Socializing with the neighbors: stem cells and their niche. Cell, 116(6), 769-778.

Ghassemi, T., Saghatolslami, N., Matin, M. M., Gheshlaghi, R., & Moradi, A. (2017). CNT-decellularized cartilage hybrids for tissue engineering applications. Biomedical Materials, 12(6), 065008.

Giovanniello, F., Asgari, M., Breslavsky, I. D., Franchini, G., Holzapfel, G. A., Tabrizian, M., & Amabili, M. (2023). Development and mechanical characterization of decellularized scaffolds for an active aortic graft. Acta Biomaterialia, 160, 59-72.

Gou, Y., Huang, Y., Luo, W., Li, Y., Zhao, P., Zhong, J., et al (2024). Adipose-derived mesenchymal stem cells (MSCs) are a superior cell source for bone tissue engineering. Bioactive Materials, 34, 51-63.

Gregory, C. A., Gunn, W. G., Peister, A., & Prockop, D. J. (2004). An Alizarin red-based assay of mineralization by adherent cells in culture: comparison with cetylpyridinium chloride extraction. Analytical Biochemistry, 329(1), 77-84.

Gresham, R. C. H., Bahney, C. S., & Leach, J. K. (2021). Growth factor delivery using extracellular matrix-mimicking substrates for musculoskeletal tissue engineering and repair. Bioactive Materials, 6(7), 1945-1956.

Guo, W., Chen, M., Wang, Z., Tian, Y., Zheng, J., Gao, S., et al. (2021). 3D-printed cell-free PCL-MECM scaffold with biomimetic micro-structure and micro-environment to enhance in situ meniscus regeneration. Bioactive Materials, 6(10), 3620-3633.

Haghighitalab, A., Matin, M. M., Amin, A., Minaee, S., Bidkhori, H. R., Doeppner, T. R., & Bahrami, A. R. (2021). Investigating the effects of IDO1, PTGS2, and TGF-β1 overexpression on immunomodulatory properties of hTERT-MSCs and their extracellular vesicles. Scientific Reports, 11(1), 7825.

Hsieh, D. J., Srinivasan, P., Yen, K. C., Yeh, Y. C., Chen, Y. J., Wang, H. C., & Tarng, Y. W. (2021). Protocols for the preparation and characterization of decellularized tissue and organ scaffolds for tissue engineering. Biotechniques, 70(2), 107-115.

Iranpour, S., Mahdavi-Shahri, N., Miri, R., Hasanzadeh, H., Bidkhori, H. R., Naderi-Meshkin, H., Zahabi, E., & Matin, M. M. (2018). Supportive properties of basement membrane layer of human amniotic membrane enable development of tissue engineering applications. Cell and Tissue Banking, 19(3), 357-371.

Jackson, D. W., Grood, E. S., Wilcox, P., Butler, D. L., Simon, T. M., & Holden, J. P. (1988). The effects of processing techniques on the mechanical properties of bone-anterior cruciate ligament-bone allografts. An experimental study in goats. The American Journal of Sports Medicine, 16(2), 101-105.

Jambar Nooshin, B., Tayebi, T., Babajani, A., Khani, M. M., & Niknejad, H. (2023). Effects of different perfusing routes through The portal vein, hepatic vein, and biliary duct on whole rat liver decellularization. Cell Journal, 25(1), 35-44.

Jasim, S. A., Yumashev, A. V., Abdelbasset, W. K., Margiana, R., Markov, A., Suksatan, W., et al. (2022). Shining the light on clinical application of mesenchymal stem cell therapy in autoimmune diseases. Stem Cell Research & Therapy, 13(1), 101.

Junqueira, L., Carneiro, J., & Kelley, R. (1998). Basic histology. 9th. Stamford, Conn.: Appleton & Lange. x.

Junqueira, L., Montes, G., & Sanchez, E. (1982). The influence of tissue section thickness on the study of collagen by the Picrosirius-polarization method. Histochemistry, 74(1), 153-156.

Kamalvand, M., Biazar, E., Daliri-Joupari, M., Montazer, F., Rezaei-Tavirani, M., & Heidari-Keshel, S. (2021). Design of a decellularized fish skin as a biological scaffold for skin tissue regeneration. Tissue and Cell, 71, 101509.

Kapuscinski, J. (1995). DAPI: a DNA-specific fluorescent probe. Biotechnic & Histochemistry, 70(5), 220-233.

Kazemi, T., Mohammadpour, A. A., Matin, M. M., Mahdavi-Shahri, N., Dehghani, H., & Kazemi Riabi, S. H. (2021). Decellularized bovine aorta as a promising 3D elastin scaffold for vascular tissue engineering applications. Regenerative Medicine, 16(12), 1037-1050.

Kersey, A. L., Cheng, D. Y., Deo, K. A., Dubell, C. R., Wang, T. C., Jaiswal, M. K., et al. (2024). Stiffness assisted cell-matrix remodeling trigger 3D mechanotransduction regulatory programs. Biomaterials, 306, 122473.

Khakpour, E., Tavassoli, A., Mahdavi-Shahri, N., & Matin, M. M. (2023). Assessing the biocompatibility of bovine tendon scaffold, a step forward in tendon tissue engineering. Cell and Tissue Banking, 24(1), 11-24.

Kiernan, J. (2008). Histological and histochemical methods: theory and practice. 4th. Bloxham, UK: Scion.

Kim, H. S., Jang, J., Oh, J. S., Lee, E. J., Han, C. M., & Shin, U. S. (2023). Injectable remodeling hydrogels derived from alendronate-tethered alginate calcium complex for enhanced osteogenesis. Carbohydrate Polymers, 303, 120473.

Komori, T. (2025). Bone development by Hedgehog and Wnt signaling, Runx2, and Sp7. Journal of Bone and Mineral Metabolism, 43(1), 33-38.

Kondo, S., Nakagawa, Y., Mizuno, M., Katagiri, K., Tsuji, K., Kiuchi, S., et al. (2019). Transplantation of aggregates of autologous synovial mesenchymal stem cells for treatment of cartilage Defects in the femoral condyle and the femoral groove in microminipigs. The American Journal of Sports Medicine, 47(10), 2338-2347.

Kostecka, A., Kalamon, N., Skoniecka, A., Koczkowska, M., Skowron, P. M., Piotrowski, A., & Pikuła, M. (2024). Adipose-derived mesenchymal stromal cells in clinical trials: Insights from single-cell studies. Life Sciences, 351, 122761.

Kubo, Y., Kaidzu, S., Nakajima, I., Takenouchi, K., & Nakamura, F. (2000). Organization of extracellular matrix components during differentiation of adipocytes in long-term culture. In Vitro Cellular & Developmental Biology – Animal, 36(1), 38-44.

Kuhbier, J. W., Weyand, B., Radtke, C., Vogt, P. M., Kasper, C., & Reimers, K. (2010). Isolation, characterization, differentiation, and application of adipose-derived stem cells. Advances in Biochemical Engineering and Biotechnology, 123, 55-105.

Lian, J. B., Morris, S., Faris, B., Albright, J., & Franzblau, C. (1973). The effects of acetic acid and pepsin on the crosslinkages and ultrastructure of corneal collagen. Biochimica et Biophysica Acta, 328(1), 193-204.

Lichtenberg, A., Tudorache, I., Cebotari, S., Ringes-Lichtenberg, S., Sturz, G., Hoeffler, K., et al. (2006). In vitro re-endothelialization of detergent decellularized heart valves under simulated physiological dynamic conditions. Biomaterials, 27(23), 4221-4229.

Lillie, R. D., Pizzolato, P., & Donaldson, P. T. (1976). Nuclear stains with soluble metachrome metal mordant dye lakes. The effect of chemical endgroup blocking reactions and the artificial introduction of acid groups into tissues. Histochemistry, 49(1), 23-35.

Luo, L., Eswaramoorthy, R., Mulhall, K. J., & Kelly, D. J. (2015). Decellularization of porcine articular cartilage explants and their subsequent repopulation with human chondroprogenitor cells. Journal of the Mechanical Behavior of Biomedical Materials, 55, 21-31.

Milan, P. B., Amini, N., Joghataei, M. T., Ebrahimi, L., Amoupour, M., Sarveazad, A., Kargozar, S., & Mozafari, M. (2020). Decellularized human amniotic membrane: From animal models to clinical trials. Methods, 171, 11-19.

Mo, M., Wang, S., Zhou, Y., Li, H., & Wu, Y. (2016). Mesenchymal stem cell subpopulations: phenotype, property and therapeutic potential. Cellular and Molecular Life Sciences, 73(17), 3311-3321.

Na, J., Yang, Z., Shi, Q., Li, C., Liu, Y., Song, Y., et al. (2024). Extracellular matrix stiffness as an energy metabolism regulator drives osteogenic differentiation in mesenchymal stem cells. Bioactive Materials, 35, 549-563.

Naderi-Meshkin, H., Matin, M. M., Heirani-Tabasi, A., Mirahmadi, M., Irfan-Maqsood, M., Edalatmanesh, M. A., et al. (2016). Injectable hydrogel delivery plus preconditioning of mesenchymal stem cells: exploitation of SDF-1/CXCR4 axis toward enhancing the efficacy of stem cells' homing. Cell Biology International, 40(7), 730-741.

Nakajima, I., Muroya, S., Tanabe, R., & Chikuni, K. (2002). Extracellular matrix development during differentiation into adipocytes with a unique increase in type V and VI collagen. Biology of the Cell, 94(3), 197-203.

Nyström, A., & Bruckner-Tuderman, L. (2019). Matrix molecules and skin biology. Seminars in Cell and Developmental Biology, 89, 136-146.

Ono, K., Hata, K., Nakamura, E., Ishihara, S., Kobayashi, S., Nakanishi, M., et al. (2021). Dmrt2 promotes transition of endochondral bone formation by linking Sox9 and Runx2. Communications Biology, 4(1), 326.

Pesaraklou, A., Mahdavi-Shahri, N., Hassanzadeh, H., Ghasemi, M., Kazemi, M., Mousavi, N. S., & Matin, M. M. (2019). Use of cerium oxide nanoparticles: a good candidate to improve skin tissue engineering. Biomedical Materials, 14(3), 035008.

Piera-Velazquez, S., Jimenez, S. A., & Stokes, D. (2002). Increased life span of human osteoarthritic chondrocytes by exogenous expression of telomerase. Arthritis & Rheumatism, 46(3), 683-693.

Porzionato, A., Sfriso, M. M., Pontini, A., Macchi, V., Petrelli, L., Pavan, P. G., Natali, A. N., et al. (2015). Decellularized human skeletal muscle as biologic scaffold for reconstructive surgery. International Journal of Molecular Sciences, 16(7), 14808-14831.

Ramírez-Zacarías, J. L., Castro-Muñozledo, F., & Kuri-Harcuch, W. (1992). Quantitation of adipose conversion and triglycerides by staining intracytoplasmic lipids with Oil red O. Histochemistry, 97(6), 493-497.

Ritter, N. M., Farach-Carson, M. C., & Butler, W. T. (1992). Evidence for the formation of a complex between osteopontin and osteocalcin. Journal of Bone and Mineral Research, 7(8), 877-885.

Roth, S. P., Erbe, I., & Burk, J. (2018). Decellularization of large tendon specimens: combination of manually performed freeze-thaw cycles and detergent treatment. Methods in Molecular Biology, 1577, 227-237.

Santoro, A., Grimaldi, M., Marino, C., Napolitano, E., Buonocore, M., & D'Ursi, A. M. (2025). Cell Surface Markers of Mesenchymal Stem Cells: Current Knowledge and Advances in Characterization Technologies. Life (Basel), 16(1).

Sarangthem, V., Sharma, H., Mendiratta, M., Sahoo, R. K., Park, R. W., Kumar, L., et al. (2022). Application of bio-active elastin-like polypeptide on regulation of human mesenchymal stem cell behavior. Biomedicines, 10(5).

Seddon, A. M., Curnow, P., & Booth, P. J. (2004). Membrane proteins, lipids and detergents: not just a soap opera. Biochimica et Biophysica Acta – Biomembranes, 1666(1-2), 105-117.

Shahabipour, F., Mahdavi-Shahri, N., Matin, M. M., Tavassoli, A., & Zebarjad, S. M. (2013). Scaffolds derived from cancellous bovine bone support mesenchymal stem cells' maintenance and growth. In Vitro Cellular & Developmental Biology – Animal, 49(6), 440-448.

Shahraki, S., Bideskan, A. E., Aslzare, M., Tavakkoli, M., Bahrami, A. R., Hosseinian, S., et al. (2022). Decellularization with triton X-100 provides

a suitable model for human kidney bioengineering using human mesenchymal stem cells. Life Sciences, 295, 120167.

Shelar, S., Gupta, U., Kumari, M., Shabib, M., Guchhait, B., Mandal, C., Kaity, S., & Roy, S. (2025). Hybrid photo-crosslinked decellularized extracellular matrix scaffold from porcine Achilles tendon: a biocompatible and non-immunogenic matrix for tissue engineering. Journal of Materials Chemistry B, 13(37), 11722-11738.

Song, J. J., & Ott, H. C. (2011). Organ engineering based on decellularized matrix scaffolds. Trends in Molecular Medicine, 17(8), 424-432.

Soták, M., Rajan, M. R., Clark, M., Biörserud, C., Wallenius, V., Hagberg, C. E., & Börgeson, E. (2022). Healthy subcutaneous and omental adipose tissue is associated with high expression of extracellular matrix components. International Journal of Molecular Sciences, 23(1), 520.

Stukel Shah, J. M., Lundquist, B., Macaitis, J., Pfau-Cloud, M. R., Beltran, F. O., Grunlan, M. A., et al. (2022). Comparative evaluation of mesenchymal stromal cell growth and osteogenic differentiation on a shape memory polymer scaffold. Journal of Biomedical Materials Research Part B: Applied Biomaterials, 110(9), 2063-2074.

Tavassoli, A., Matin, M. M., Niaki, M. A., Mahdavi-Shahri, N., & Shahabipour, F. (2015). Mesenchymal stem cells can survive on the extracellular matrix-derived decellularized bovine articular cartilage scaffold. Iranian Journal of Basic Medical Sciences, 18(12), 1221-1227.

Waldrop, F. S., Puchtler, H., Meloan, S. N., & Younker, T. D. (1980). Histochemical investigations of different types of collagen. Acta Histochemica Supplement, 21, 23-31.

Wang, D., Pun, C. C. M., Huang, S., Tang, T. C. M., Ho, K. K. W., Rothrauff, B. B., et al. (2020). Tendon-derived extracellular matrix induces mesenchymal stem cell tenogenesis via an integrin/transforming growth factor-β crosstalk-mediated mechanism. FASEB Journal, 34(6), 8172-8186.

Wang, Y., Zhang, W., & Yao, Q. (2021). Copper-based biomaterials for bone and cartilage tissue engineering. Journal of Orthopaedic Translation, 29, 60-71.

Wen, Q., Mithieux, S. M., & Weiss, A. S. (2020). Elastin biomaterials in dermal repair. Trends in Biotechnology, 38(3), 280-291.

Yang, B., Zhang, Y., Zhou, L., Sun, Z., Zheng, J., Chen, Y., & Dai, Y. (2010). Development of a porcine bladder acellular matrix with well-preserved extracellular bioactive factors for tissue engineering. Tissue Engineering Part C: Methods, 16(5), 1201-1211.

Yang, Q., Di, T., Zhang, G., Luo, X., Zhu, Y., Wen, Y., et al. (2025). A novel polyurethane nanofiber scaffold with mechanical adaptability and anti-adhesion properties promotes tendon regeneration. Biomaterials Advances, 180, 214536.

Zhang, J., Li, B., & Wang, J. H. (2011). The role of engineered tendon matrix in the stemness of tendon stem cells in vitro and the promotion of tendon-like tissue formation in vivo. Biomaterials, 32(29), 6972-6981.

Zhang, Z., Luo, X., Xu, H., Wang, L., Jin, X., Chen, R., et al. (2015). Bone marrow stromal cell-derived extracellular matrix promotes osteogenesis of adipose-derived stem cells. Cell Biology International, 39(3), 291-299.

Zorlutuna, P., Vrana, N. E., & Khademhosseini, A. (2013). The expanding world of tissue engineering: the building blocks and new applications of tissue engineered constructs. IEEE Reviews in Biomedical Engineering, 6, 47-62.

Open Access Statement:
This is an open access article distributed under the Creative Commons Attribution License (CC-BY), which permits unrestricted use, distribution, and reproduction in any medium, provided the original work is properly cited.

Supplementary data

Table S1. Number of adipose-derived mesenchymal stem cells after 48 hours on plastic surface and biomatrix (Cells were cultured in 6-well plates with a culture area of 9.5 cm^2)

	Well 1 (Replicate 1)	**Well 2 (Replicate 2)**	**Well 3 (Replicate 3)**	**Mean cell number**
Plastic surface	225000	210000	187500	207500
Biomatrix	337500	322500	300000	320000

Table S2. Optical density (OD) values after Alizarin Red S staining at days 7, 14, and 21, for osteogenic differentiation (cells were cultured in 6-well plates with a culture area of 9.5 cm^2)

Time after induction (days)	**ODM (Osteogenic differentiation medium)**	**Osteogenic differentiation medium + Biomatrix**
7	0.05	0.09
14	0.37	1.07
21	0.66	1.49

Table S3. Optical density (OD) values after Oil Red O staining at days 7, 14, and 21, for adipogenic differentiation (cells were cultured in 6-well plates with a culture area of 9.5 cm^2)

Time after induction (days)	**ADM (Adipogenic differentiation medium)**	**Adipogenic differentiation medium + Biomatrix**
7	0.125	0.156
14	0.321	0.493
21	0.633	0.860